

ULRR

Analysis of skin recovery from mechanical indentation using diffuse lighting and digital imaging

Item Type	Meetings and Proceedings
Authors	Clancy, Neil T.; Leahy, Martin J.; Nilsson, Gert E.; Anderson, Chris
Citation	Diffuse Optical Imaging of Tissue;6629/ 66291G
Publisher	Society of Photo-Optical Instrumentation Engineers (SPIE)
Download date	2026-05-14 01:58:29
Item License	https://creativecommons.org/licenses/by-nc-sa/1.0/
Link to Item	https://hdl.handle.net/10344/129

Analysis of skin recovery from mechanical indentation using diffuse lighting and digital imaging

Neil T. Clancy*^a, Martin J. Leahy^a, Gert E. Nilsson^b, Chris Anderson^c

^aDepartment of Physics, University of Limerick, Ireland;

^bInstitutionen för medicinsk teknik, Linköpings universitet, SE - 581 82 Linköping, Sweden;

^cInstitutionen för biomedicin och kirurgi, Linköpings universitet, Linköping, Sweden.

ABSTRACT

Skin behaves as a viscoelastic material, having mechanical properties composed of elastic and fluid components. Upon indentation, the fibres are stretched and fluid displaced from the compressed region. The rate of recovery from this imprint is therefore dependent on the hydration and elasticity of the skin. A reliable measurement could be applied to the assessment of clinical conditions such as oedema, rare genetic disorders such as *cutis laxa* and the evaluation of the ‘effective age’ of skin *in vivo*. This paper describes a new approach to the non-invasive indentation technique and a novel method of analysis. A method is proposed that tracks the skin’s recovery optically from an initial strain made using a mechanical indenter, diffuse side-lighting and a CCD video-capture device. Using the blue colour plane of the image it is possible to examine the surface topography only, and track the decay of the imprint over time. Two algorithms are discussed for the extraction of information on the skin’s displacement and are analysed in terms of reliability and reproducibility.

Keywords: Indentation method, viscoelasticity, oedema, skin, image analysis, diffuse lighting.

1. INTRODUCTION

The viscoelastic properties of human skin are due to the contributions of various elastic materials, the ground substance and the extracellular fluid. In the skin, the most linearly elastic material, elastin is present as thin strands and makes up approximately 4% of dry skin mass [1]. A small amount of hysteresis exists in loading and unloading cycles indicating energy dissipation in the material. The linearity remains up to strain values of 1.6. Collagen is the basic structural material for both soft and hard tissues in the human body, serving as a supporting element for the extracellular matrix, transmitting and dissipating loads, preventing premature mechanical failure, partitioning cells and tissues into functional units and constitutes approximately 75% of dry skin mass [1-3]. The intracellular space is filled with fibres of collagen, elastin, reticulin and ground substance – a hydrophilic gel. Loose connective tissue especially contains a lot of this water-based substance. The exact composition varies but contains mucopolysaccharides (glycosaminoglycans) and tissue fluid [1]. The mobility of water within this gel has a large impact on the mechanical properties of the tissue [4-8].

A knowledge of the mechanical properties of the skin is essential in assessing clinical conditions such as oedema which can arise from trauma to the tissue (burns, injury) or blockages in the lymph system (cancer) [9]. A reliable measurement of the elastic components could similarly prove useful in the diagnosis of genetic conditions affecting the elastin gene such as *cutis laxa*.

The use of mechanical stimuli to extract information on the viscoelastic nature of human skin has been investigated previously [4, 6, 10]. Typical experiments were of the ‘stress relaxation’ type – measuring the decay of force needed to maintain an imprint of certain depth i.e., constant strain. These were based on the principle that as the indenter pressed against the skin, the elastic fibres were stretched and interstitial fluid displaced from the region under compression. Other techniques that measure the recovery of skin after indentation require the use of linear variable differential transformers and constant mechanical contact with the skin [11].

This paper describes an optical approach to measuring skin recovery after indentation that is non-invasive and non-contact. After indentation, the skin recovers to its original state as the elastic fibres recoil and fluid returns to the compressed region. The rate of this recovery is therefore dependent on the local mechanical properties of the tissue.

*neil.clancy@ul.ie; phone +35361 202307

A reproducibility test was conducted on the volar forearm of a healthy volunteer and the results analysed using two different algorithms to determine the optimum technique. Using this method, the forearm skin of a volunteer was tested after insertion of a microdialysis probe. It has been shown that the skin has a short-lived axon reflex mediated inflammatory response to the trauma of catheter insertion [12, 13]. Changes other than erythema have not previously been quantified. The ability to quantify the degree of tissue swelling around the microdialysis membrane would have importance in the modelling of microdialysis data. The results of the indentation test trialled here should reveal whether there is any oedema present and allow quantification of its degree.

2. THEORY

In order to quantify the viscous and elastic properties of a material such as skin, it is useful to develop a mechanical analogue of the situation. Here, the well-known Kelvin-Voigt model is applied [14], consisting of a purely elastic component (spring of Young's modulus E) and a purely viscous component (dashpot with fluid of viscosity η) arranged in parallel as shown in figure 1.

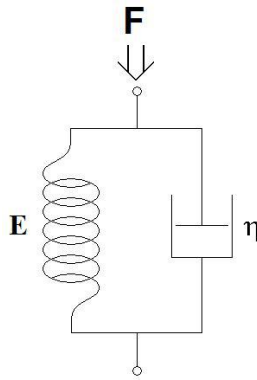


Fig. 1. Kelvin-Voigt model of viscoelasticity. The spring and dashpot are arranged in parallel to allow the element to recover after the force 'F' has been removed. The spring has Young's modulus 'E' while the dashpot contains fluid of viscosity 'η'.

As shown in figure 1 above, when the force 'F' is applied, both elements experience the same strain while the stress is the sum of the stresses in the individual components:

$$\sigma(t) = \varepsilon(t)E + \eta \frac{d\varepsilon(t)}{dt} \quad (1)$$

where σ is stress, ε is strain and t is time.

If the compressive force is released at a certain time, the above equation becomes:

$$0 = \varepsilon E + \eta \frac{d\varepsilon}{dt}$$

Rearranging,

$$\frac{d\varepsilon}{dt} + \frac{E}{\eta} \varepsilon = 0$$

This is a simple first order ordinary differential equation with a standard solution resulting in an expression for ε :

$$\varepsilon(t) = Ce^{-\frac{E}{\eta}t} \quad (2)$$

If the stress is removed at $t = 0$, the material is left at some initial strain ε' :

$$\begin{aligned} \varepsilon(0) = \varepsilon' &= Ce^{-\frac{E}{\eta}(0)} \\ \Rightarrow C &= \varepsilon' \\ \therefore \varepsilon(t) &= \varepsilon' e^{-\frac{E}{\eta}t} \end{aligned}$$

The time constant is defined as $\tau = \frac{E}{\eta}$, giving the final result:

$$\varepsilon(t) = \varepsilon' e^{-\frac{t}{\tau}} \quad (3)$$

This shows that if an imprint is made in a viscoelastic material, the size of that imprint will decay exponentially once the stress has been removed. As mentioned in section 1, water in the tissue may be present as free-flowing fluid or enmeshed in ground substance. This means that more than one value of viscosity must be considered. This can be incorporated into the above model by addition of a second dashpot in series with the first. This results in a new expression for strain:

$$\varepsilon(t) = C_1 e^{-\frac{t}{\tau_1}} + C_2 e^{-\frac{t}{\tau_2}} \quad (4)$$

where C_1 and C_2 are the fractional amounts of each fluid and τ_1 and τ_2 are the time constants for the decay corresponding to each type.

3. METHODOLOGY

3.1 Background

The technique used is a variation on the impression method employed previously in studies of oedema [5, 15]. However, in this case the measurement principle is to measure the decay of a mechanical imprint in the skin and from the rate of this decay, extract information on its viscoelastic properties.

The impression is made mechanically by pressing a suitable indenter against the skin, displacing it by 3 mm. The skin is kept at this constant strain for 20 seconds (based on previous studies of fluid translocation [4]). When this is done, fluid in the interstitial space is 'squeezed' from the area under compression (viscous response) and collagen and elastin fibres are stretched (elastic response). When the indenter is removed, the elastic fibres 'recoil' to their original state, the fluid moves back into the compressed area and the imprint disappears. The response of the skin to this stimulus is a function of its condition i.e., hydration, age, physiological conditions. To quantify this response, a digital camera method is proposed whereby images of the impression are acquired over time and through appropriate algorithms, a graph of imprint decay is obtained. By comparing different decay curves it should be possible to differentiate skin at different stages of oedema and varying elasticity.

To achieve this, a suitable method of lighting the imprint must be chosen. A side-illumination scheme (figure 2) leads to a shadow in the imprinted area proportional to the size of the imprint itself. As the skin recovers to its undisturbed state, the shadow area also decreases. Tracking the shadow area over time using a digital video camera therefore enables quantification of the viscoelastic properties of the skin as predicted in section 2. The indenter is incorporated in the lighting ring allowing imaging of the imprint immediately after the indenter is removed.

Another factor to be taken into account is the surface area of skin that is under compression. When areas of 2 mm² or less are imprinted, tissue fluid is dispersed from the upper dermis. However, when larger areas i.e., 1 cm² or more, are

compressed, lymphatics may also be involved allowing fluid to be squeezed out of the deep dermis, accumulating in the upper dermis [16]. Therefore, a small indenter (1 mm wide) was chosen for this study.

A linear-shaped indenter was chosen as it offered a number of advantages including simplicity, ease of manufacture and potential to adapt to different analyses. The indenter and lighting system is shown in figure 2. The diffuse side-illumination scheme is powered by a 6.5 W tungsten halogen source, transported to the lighting 'ring' using 1 mm core diameter polymer optical fibres. The lighting ring itself is clear Perspex with a bevelled edge to reflect the light horizontally while a coat of white diffusely reflecting paint on the outer surface ensures an even illumination.



Fig. 2. Indenter and lighting system. The diffuse lighting ring and indenter are attached to the lens assembly of the camera. The base plate ensures even, low pressure contact with the skin and a flat region of interest. The indenter recoils from the field-of-view after the impression time (20 s) has elapsed.

The images were acquired using a commercially available digital video camera (Panasonic nvgs150). A frame-grabbing routine written in Matlab (© The Math Works) acquired raw images at 25 Hz from a user-specified region-of-interest (250 x 250 pixels).

The indenter and lighting ring were attached to the lens assembly of the camera as shown in figure 2. Prior to measurement, the indenter was placed in the downward position. The entire device was then lowered until the base plate made even contact with the skin. The indenter was left in place for 20 seconds to allow the imprint to form, and image acquisition was initiated. The release catch was then opened allowing the indenter to spring back from the skin, exposing the imprint to the camera.

Image processing was carried out using custom-written Matlab programs. Two different approaches are described here.

3.2 Thresholding

The raw colour (RGB) images are separated into the red, green and blue planes. To reduce the effect of light contributions from deeper in the tissue and concentrate on the surface topography, the blue colour plane is used. Confounding effects due to variations in ambient light and fluctuations in the output power of the source are limited by normalising each image by the average of the three colour planes.

The resulting greyscale image is then converted to binary (black and white) using an appropriate threshold value (figure 3). This is calculated automatically using an in-built Matlab routine that uses an algorithm developed by Otsu [17] to maximise the inter-class variance based on a histogram of the greyscale levels in the image. This isolates the shadow of the imprint from the background and the binary image is then created from the threshold value (greyscale values less than the threshold are black, those equal to or above it become white).

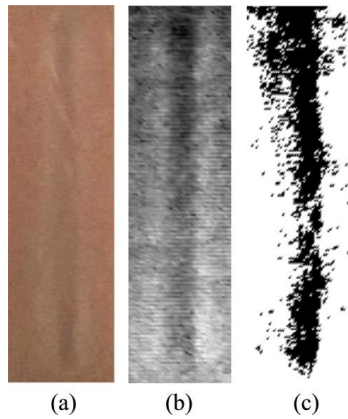


Fig. 3. Thresholding processing steps. The raw image (a) is converted to greyscale by normalising the blue plane by the average greyscale value across the red, green and blue planes (b). The threshold is calculated based on the histogram of greyscale values in this image, from which the binary image (c) results.

3.3 Greyscale profile

The image is normalised as above, once again using the blue colour plane. As the greyscale values decrease in darker areas, a cross-section of the image will yield a characteristic ‘trough’ shape in the region of the imprint. By averaging along the length of the imprint, an average greyscale profile can be generated. A ‘Mexican hat’ waveform, common in wavelet analysis and described by equation 5, was found to be a good fit to the data (figure 4).

$$\text{greyscale value} = -A \left(1 - \left(\frac{x}{B} \right)^2 \right) e^{-\left(\frac{x}{B\sqrt{2}} \right)^2} + C \quad (5)$$

where A and B are constants relating to the depth and width, and C is an offset.

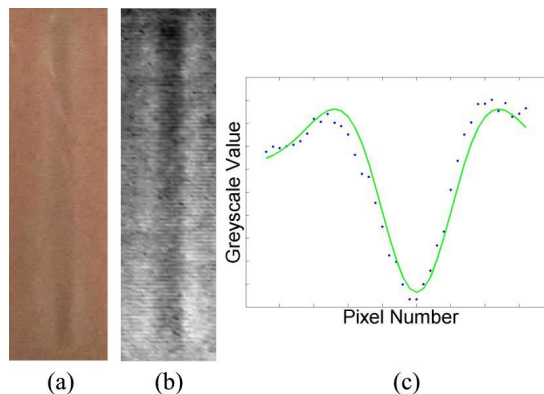


Fig. 4. Greyscale profile. The raw image (a) is normalised as before (b), the average greyscale values are calculated along the length of the imprint and the ‘Mexican hat’ equation described in equation 5 is fitted to the data (c) using an iterative method that minimises the rms error. The fit parameters can then be used to calculate the ‘depth’ of the shadow.

From the fit parameters, the ‘depth’ of the profile can be readily calculated, as shown in equation 6 below.

$$'Depth' = A \left(2e^{-\frac{3}{2}} + 1 \right) - C \quad (6)$$

A decay curve for the imprint can then be generated by plotting greyscale depth against time.

4. RESULTS

Four consecutive indentation tests were carried out on the volar forearm of a 25 year-old male on a 9 cm² area of skin. The raw images were processed using the thresholding and greyscale profile methods outlined above.

4.1 Thresholding

Figure 5 shows a typical data set obtained using the thresholding method. In the first 15 seconds, the imprint index increases. This is due to capillary refilling in the region of the imprint. After this, the imprint recovers as predicted, following the biexponential decay.

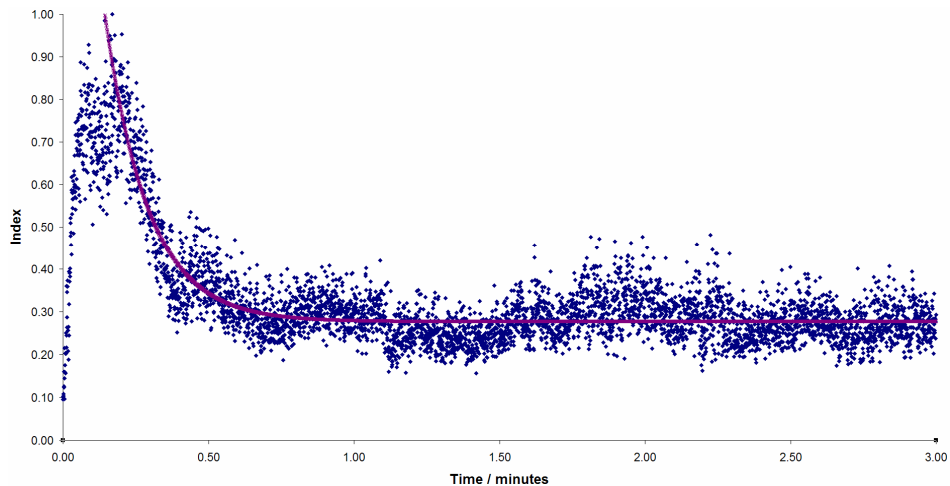


Fig. 5. Thresholding decay data and fit. The imprint decays in a biexponential fashion as predicted. The first 15 seconds show an apparent increase in imprint size due to capillary refilling. The index is normalised by the maximum imprint size.

The decay curves for the reproducibility tests are shown in Figure 6. On visual inspection, the curves all show a similar shape in the first 30 seconds. All four reach a steady non-zero baseline value within the 3 minute test.

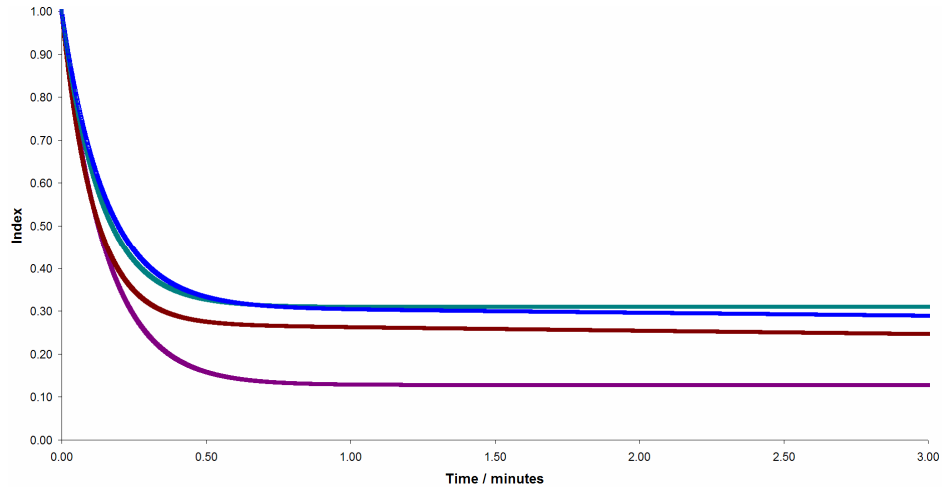


Fig. 6. Reproducibility test – thresholding. Each curve decays to a steady state value within 3 minutes, with each settling at a different offset value.

The parameters for the decay are listed in table 1. The average values of τ_1 and τ_2 were 14346.91 ± 22634.51 minutes (157% variation) and 0.14 ± 0.02 minutes (15% variation) respectively while the corresponding fractional constants C_1 and C_2 were 0.43 ± 0.11 (26% variation) and 1.33 ± 0.42 (32% variation).

Table 1. Time and fractional constants for the decay curves generated using the thresholding method.

Test no.	C_1	C_2	τ_1 / minutes	τ_2 / minutes
1	0.28	1.90	45300.83	0.15
2	0.46	1.25	31.80	0.11
3	0.50	1.11	12013.34	0.14
4	0.47	1.05	41.67	0.15

4.2 Greyscale Profile

A high degree of reproducibility is noticed immediately in the tight grouping of the decay curves (figure 7).

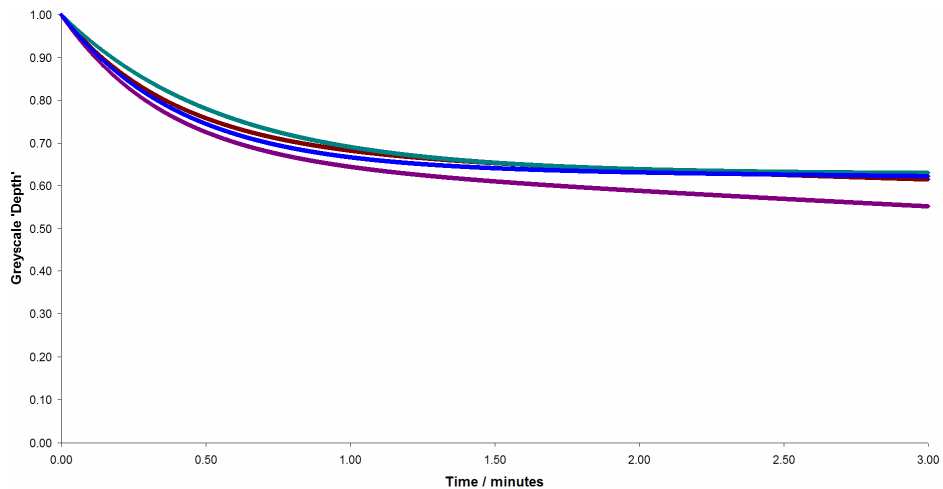


Fig. 7. Reproducibility test – greyscale profile. Decay curves representing four indentation tests were conducted on the volar forearm skin of a 25 year-old male. The greyscale 'depth' is normalised by the maximum value.

The curves do not level off within the three minute period this time, as expected. The parameters for the curves are listed in table 2.

Table 2. Constants relating to the decay curves generated using the greyscale profile algorithm.

Test no.	C_1	C_2	τ_1 / minutes	τ_2 / minutes
1	0.33	0.65	0.35	16.19
2	0.30	0.63	0.40	30.32
3	0.37	0.63	0.56	1755.05
4	0.36	0.64	0.41	101.88

The average values for the time constants τ_1 and τ_2 were 0.43 ± 0.10 minutes (24% variation) and 475.86 ± 869.43 minutes (183% variation) while C_1 and C_2 were 0.34 ± 0.04 (11% variation) and 0.64 ± 0.01 (1% variation).

4.3 Microdialysis

A microdialysis probe was inserted in the forearm epidermis of a healthy 25 year-old male volunteer as described in section 1 and an indentation test was carried out immediately ($t = 0$ minutes). Further indentations were made at $t = 90$ minutes, 6 hours and 24 hours. Following the evaluation of the algorithms, only the greyscale profile method was used to process the results. The decay curves at each point in time are shown in figure 8.

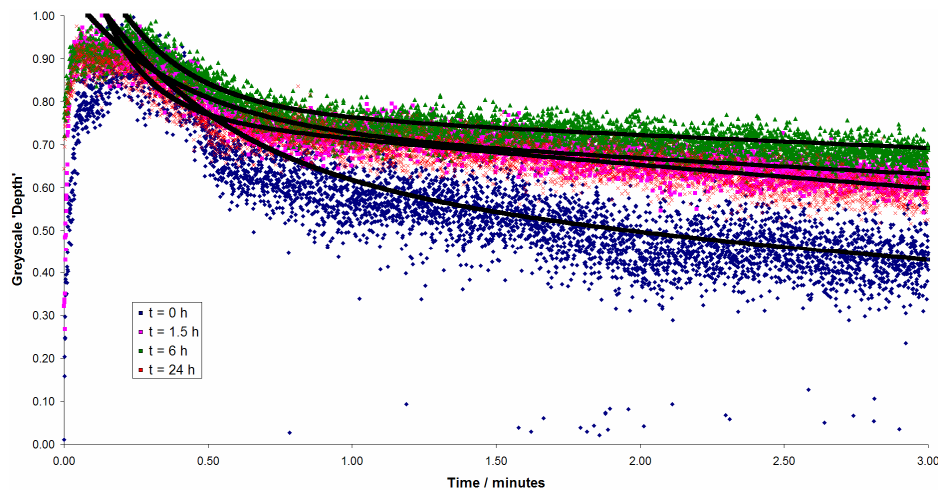


Fig. 8. Microdialysis test. The first imprint was made immediately after insertion of the probe with successive tests at 90 minutes, 6 hours and 24 hours. Recovery time increased with test time with the exception of the final (24 hour) imprint.

The parameters characterising each curve are given in table 3 and show that the fraction of fluid increased along with a corresponding increase in τ_2 .

Table 3. Fit parameters for microdialysis test results. The fraction of high viscosity fluid, C_2 increased over the course of the experiment. There was a corresponding increase in the time constant for the decay in τ_2 with the exception of the final 24 hour test.

Test Time / hours	C_1	C_2	τ_1 / minutes	τ_2 / minutes
0	0.52	0.64	0.46	7.56
1.5	0.33	0.74	0.37	17.95
6	0.52	0.79	0.26	23.62
24	0.57	0.78	0.16	11.46

5. DISCUSSION

5.1 Decay Curve Analysis

The blue colour plane was chosen for analysis purposes as wavelengths in this region (approximately 400 – 500 nm) have significantly shallower penetration depths than longer wavelengths. Therefore, the image would contain information on the surface of the skin. However, the initial 15 seconds of data in the decay curve show an apparent increase in imprint size. This corresponds to the refilling time of capillaries that had been occluded by the indenter. Due to the wide range of wavelengths in the camera's blue CCD (400 – 500 nm) however, some light containing information on the microvasculature does reach the detector. A possible solution to this problem is to use polarisation gating with a filter over the camera lens orientated parallel to a polarised light source. Only superficially or specularly reflected photons maintaining their polarisation would then be allowed through the filter whilst the depolarised photons arriving from blood vessels deeper in the tissue would be rejected.

5.2 Reproducibility

The decay curves generated using the thresholding method tend toward a steady state (plus an offset, due to shadows not related to the imprint) more rapidly than those of the greyscale profile method. This depends largely on the threshold chosen. Small variations in lighting and placement of the imprint with respect to the illumination ring can result in the calculation of an erroneously low threshold value. This means that pixels in the imprint area are assigned the value '1' more quickly than expected and the signal-to-noise ratio is decreased. The result is that these curves suggest that the imprint disappears completely after approximately 1 minute, which is not supported by observations that show the imprint is still partially visible several minutes after indentation. The greyscale profile decay curves paint a more realistic picture with τ_2 values of the order of 20 minutes (with the exception of one outlier), supporting observations.

5.3 Response to Microdialysis

As mentioned in section 1, if tissue suffers a trauma (in this case the insertion of a dermal catheter), leakage of fluid to the interstitial space will occur and a localised oedema will form. This experiment sought to determine if this predicted oedema could be detected using the indentation technique. The results shown in figure 8 and table 3 indicate that this is indeed possible. The parameter C_2 (representing higher viscosity fluid and the 'tail' of the decay curve) increases over the measurement period. The time constant τ_2 shows a corresponding increase in the first 6 hours after insertion of the probe. However, the 24 hour measurement shows a drop to a near-baseline level. This may reflect tissue equilibration from the insertion trauma (in the same fashion as recovery from the axon reflex-based erythematous response seen in previous work [12]). Another possible explanation is that the probe tip may have moved during the latter (overnight) part of catheter placement which might have allowed the swelling in the area to decrease. Further study will confirm the phenomenon and the possibility for quantification of the amount of swelling, which in turn could be factored into modelling of microdialysis data.

6. CONCLUSIONS

The mechanical response of the skin is in agreement with the simple viscoelastic model described. The size of a mechanical imprint in the skin decays in a biexponential fashion as predicted.

Two different algorithms have been examined. It was found that the thresholding method, despite being faster computationally, led to an erroneous interpretation of the state of the tissue underestimating skin recovery time. The greyscale profile algorithm fits a curve to the average greyscale values across the imprint. This results in decay curves that match the actual response time of the skin and is less sensitive to static shadows.

The most difficult section of the decay curve to track accurately is the initial 30 seconds involving the confounding motion of low viscosity tissue fluid, capillary refilling and elastic fibre recoil. This is illustrated by the large variation in τ_1 measured. The capillary refilling in particular causes difficulties in the first 15 seconds but may be eliminated using appropriate polarisation filters.

The device is sensitive to changes in tissue water as shown by its response to oedema resulting from the insertion of a microdialysis probe in the epidermis. An increase in the fraction of high viscosity fluid present over 24 hours was recorded along with an increase in the time constant for the decay.

REFERENCES

- 1 Y. C. Fung, *Biomechanics: Mechanical Properties of Living Tissues*, Springer-Verlag, New York, 1993.
- 2 F. H. Silver, I. Horvath and D. J. Foran. "Mechanical implications of the domain structure of fibre-forming collagens: comparison of the molecular and fibrillar flexibilities of the α 1-chains found in types I-III collagen." *J. Theor. Biol.* 216, 243-254 (2002).
- 3 F. H. Silver, G. P. Seehra, J. W. Freeman and D. DeVore. "Viscoelastic properties of young and old human dermis: a proposed molecular mechanism for elastic energy storage in collagen and elastin." *J. Appl. Polym. Sci.* 86, 1978-1985 (2002).
- 4 O. A. Lindahl, K. A. Ångquist and S. Ödman. "Impression technique for the assessment of oedema - technical improvement methodological evaluation of a new technique." *Med. Biol. Eng. Comput.* 29, 591-597 (1991).
- 5 O. A. Lindahl, A. Bergh, J.-E. Damber and K. A. Ångquist. "Evaluation of the impression technique by measuring interstitial oedema in rat testis." *Acta Physiol. Scand.* 143, 255-260 (1991).
- 6 O. A. Lindahl, J. Zdolsek, F. Sjöberg and K. A. Ångquist. "Human postburn oedema measured with the impression method." *Burns.* 19(6), 479-484 (1993).
- 7 M. Mridha and S. Ödman. "Characterization of subcutaneous edema by mechanical impedance measurement." *J. Invest. Dermatol.* 85, 576-578 (1985).
- 8 H. J. Zdolsek, O. A. Lindahl and F. Sjöberg. "Non-invasive assessment of fluid volume status in the interstitium after haemodialysis." *Physiol. Meas.* 21, 211-220 (2000).
- 9 A. C. Guyton, *Textbook of Medical Physiology*, W. B. Saunders Company, Philadelphia, London, Toronto, Montreal, Sidney, Tokyo, 1991.
- 10 A. Delalleau, G. Josse, J. M. Lagarde, H. Zahouani and J. M. Bergheau. "Characterization of the mechanical properties of skin by inverse analysis combined with the indentation test." *J. Biomech.* 39(9), 1603-1610 (2006).
- 11 S. Doubal and P. Klemra. "Visco-elastic response of human skin and aging." *J. Am. Aging Assoc.* 25, 115-118 (2002).
- 12 C. Anderson, T. Andersson and K. Wårdell. "Changes in skin circulation after insertion of a microdialysis probe visualized by laser Doppler perfusion imaging." *J. Invest. Dermatol.* 102(5), 807-811 (1994).
- 13 M. Lindén, T. Andersson, K. Wårdell and C. Anderson. "Is vascular reactivity in skin predictable?" *Skin Res. Technol.* 6, 27-30 (2000).
- 14 J. J. Aklonis, W. J. MacKnight and M. Shen, *Introduction to Polymer Viscoelasticity*, John Wiley & Sons, Inc., New York, London, Sydney, Toronto, 1972.
- 15 H. J. Zdolsek, O. A. Lindahl, K. A. Ångquist and F. Sjöberg. "Non-invasive assessment of intercompartmental fluid shifts in burn victims." *Burns.* 24, 233-240 (1998).
- 16 T. J. Ryan, M. Thoolen and Y. H. Yang. "The effect of mechanical forces (vibration or external compression) on the dermal water content of the upper dermis and epidermis, assessed by high frequency ultrasound." *J. Tissue Viability.* 11(3), 97-101 (2001).
- 17 N. Otsu. "A threshold selection method from gray-level histograms." *IEEE Trans. Syst. Man Cybern.* 9(1), 62-66 (1979).